AGU PUBLICATIONS

JGR

Journal of Geophysical Research: Biogeosciences

RESEARCH ARTICLE
10.1002/2017JG004088

Key Points:
- Promotion effect of Asian dust on phytoplankton growth is confirmed by incubation experiments in the South China Sea
- Comprehensive analysis of phytoplankton growth reveals potential utilization of dissolved organic phosphorus
- Oligotrophic and ultraoligotrophic conditions were identified, leading to different phytoplankton responses to external inputs

Supporting Information:
- Supporting Information S1
- Data Set S1
- Data Set S2

Correspondence to:
H. Gao,
hwgao@ouc.edu.cn

Citation:
Chu, Q., Liu, Y., Shi, J., Zhang, C., Gong, X., Yao, X., et al. (2018). Promotion effect of Asian dust on phytoplankton growth and potential dissolved organic phosphorus utilization in the South China Sea. *Journal of Geophysical Research: Biogeosciences*, *123*, 1101–1116. https://doi.org/10.1002/2017JG004088

Received 1 AUG 2017
Accepted 7 FEB 2018
Accepted article online 14 FEB 2018
Published online 30 MAR 2018

Promotion Effect of Asian Dust on Phytoplankton Growth and Potential Dissolved Organic Phosphorus Utilization in the South China Sea

Qiang Chu[1,2], Ying Liu[1,3], Jie Shi[1,4], Chao Zhang[1], Xiang Gong[5], Xiaohong Yao[1], Xinyu Guo[1,2], and Huiwang Gao[1,4]

[1]Key Laboratory of Marine Environment and Ecology, Ocean University of China, Ministry of Education of China, Qingdao, China, [2]Center for Marine Environmental Studies, Ehime University, Matsuyama, Japan, [3]Now at College of Chemistry, Chemical & Environmental Engineering, Weifang University, Weifang, China, [4]Laboratory for Marine Ecology and Environmental Sciences, Qingdao National Laboratory for Marine Science and Technology, Qingdao, China, [5]School of Mathematics and Physics, Qingdao University of Science and Technology, Qingdao, China

Abstract Dust deposition is an important nutrient source to the South China Sea (SCS), but few in situ experiments were conducted on phytoplankton response to the deposition. We conducted onboard incubation experiments at three stations near Luzon Strait in the SCS, with addition of multiple dissolved inorganic nutrients, Asian dust, and rainwater. From our results, nitrogen and phosphorus were both urgently needed for phytoplankton growth in the SCS, indicated by the evident Chl *a* response to the addition of nitrogen and phosphorus together. Almost no evident response was observed by adding phosphorus or iron alone to incubation waters, although a delayed response of Chl *a* in mass concentration was observed by adding nitrogen alone. The latter implied a possible utilization of dissolved organic phosphorus because of insufficient dissolved inorganic phosphorus in incubation waters. Under such nutrient condition, Asian dust showed an apparent promotion effect on phytoplankton growth by providing sufficient amounts of nitrogen but low phosphorus. Meanwhile, it was found that large sized ($>$ 5 μm) phytoplankton community showed different responses to dust addition at different stations. At stations A3 and A6, *Chaetoceros* spp. became the dominant species during the bloom period, while at station WG2, *Nitzschia* spp. became dominant. In combination with different initial nutrients and Chl *a* levels at the three stations, the different phytoplankton community evolution implied the response difference to external inputs between oligotrophic (stations A3 and A6) and ultraoligotrophic (station WG2) conditions in the SCS.

1. Introduction

Atmospheric deposition is important to the ocean by providing large amount of bioavailable elements, among which dust events play a vital role (Duce et al., 2008; Jickells et al., 2005). Asian dust is reported to be one of the largest source of dust and can be transported more than thousands of kilometers eastward over the East Asian continent and the Pacific Ocean in spring (Shao et al., 2011; Zhao et al., 2003). During the transport of Asian dust, it can deposit and thereby supply bioavailable nutrients (N, P, Si, etc.) and trace metals (Fe, Mn, etc.) to the ocean, which is considered to have a significant influence on marine ecosystems (Tan et al., 2011; Wang et al., 2012). The fertilization effect of dust has been reported in oligotrophic Mediterranean Sea and Atlantic Ocean (Mills et al., 2004; Ridame et al., 2014), as well as in western North Pacific Ocean (Yuan & Zhang, 2006) and coastal China seas (Tan et al., 2011), for example, in the Yellow Sea (Shi et al., 2012) and the South China Sea (SCS) (Wang et al., 2012).

In marine ecosystems, changes in nutrient availability occur on different temporal and spatial scales, affecting elemental stoichiometry, primary production, and limiting conditions (Arrigo, 2005; Eppley & Peterson, 1979). Nitrogen is the limiting nutrient for phytoplankton growth in the low-latitude open ocean (Moore et al., 2013; Vitousek & Howarth, 1991). Iron is considered to limit phytoplankton growth in high-nutrient low-chlorophyll regions (Boyd et al., 2000; Tsuda et al., 2003). Meanwhile, iron can also be the limiting nutrient in oligotrophic regions due to its effect on nitrogen fixation (Wu et al., 2003). Phosphorus is considered to be the limiting nutrient in the Mediterranean Sea (Thingstad et al., 2005) and is treated as a secondary limiting nutrient in the open ocean (Moore et al., 2013). In addition, dissolved organic phosphorus (DOP) contributes to algae

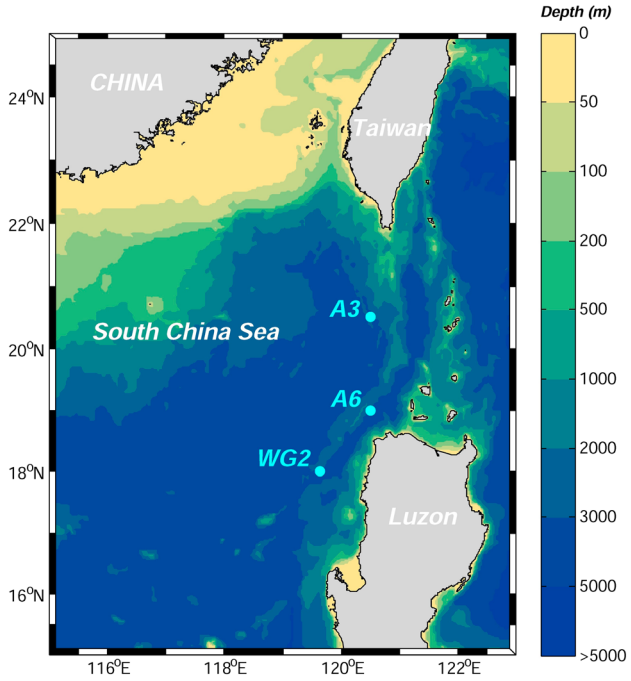

Figure 1. Sampling stations in the South China Sea.

growth in low dissolved inorganic phosphorus (DIP) concentration conditions (Lin et al., 2012; Lomas et al., 2010).

Through satellite and field observations, enhancement of primary production by atmospheric deposition has been revealed (Shi et al., 2012; Tan et al., 2011). Nutrient enrichment bioassays, especially in situ incubation experiments, are widely used to directly evaluate the limiting condition and oceanic responses to dust deposition in oligotrophic oceans (Davey et al., 2008; Giovagnetti et al., 2013; Moore et al., 2008). Some onboard incubation experiments have also been carried out in the marginal seas of China, including both shelf and basin regions, to investigate the planktonic response to nutrients and dust addition (Guo et al., 2012; Liu et al., 2013). To integrate analysis of nutrient and plankton dynamics in mesocosm incubations, models were developed in some studies for specific experiments (Thingstad et al., 2007; Van den Meersche et al., 2004). A combination of in situ experiments and models can better explain these processes in various marine ecosystems.

The SCS is one of the largest marginal seas in the world and is located in the western North Pacific Ocean (Chen et al., 2004). It is an oligotrophic region with deep euphotic zone (Wong et al., 2007). The nitracline depth (depth where dissolved inorganic nitrogen (DIN) equals 0.1 μmol/L) (Herbland et al., 1985) varies from 20 m in winter to 80 m in summer (Chen, 2005). Bordering on East Asia continent, the SCS, especially the northern part, is readily affected by Asian dust deposition mixed with anthropogenic aerosols (Wang et al., 2011) during the monsoon season (Zhang et al., 1997). The deposition of Asian dust and anthropogenic aerosols can increase biomass and primary production, promote the phytoplankton blooms, and change the phytoplankton community structure (Guo et al., 2012; Wang et al., 2012).

However, limiting conditions and the marine ecosystem response to atmospheric deposition, especially the entire processes including blooming and extinction period, remain poorly understood due to the lack of in situ studies in the SCS. In our research, we conducted onboard incubation experiments to assess the response of phytoplankton communities to nutrient, dust, and rainwater deposition in the SCS. Also, a biogeochemical box model was used to improve understanding of biological processes during incubation experiments. This study aims to (1) assess the nutrient-limiting conditions for the phytoplankton growth in the SCS and (2) investigate the effect of Asian dust on the biogeochemistry and community structure in the incubation system.

2. Materials and Methods

Onboard incubation experiments were conducted during the cruise of R/V *Dongfanghong 2* from 21 March to 2 May 2013 in the SCS. Sampling and experiments were conducted at station A3 (120.50°E, 20.50°N) starting on 27 March, at station A6 (120.50°E, 19.00°N) starting on 12 April, and at station WG2 (119.64°E, 18.00°N) starting on 23 April (Figure 1). All three sampling stations were located near the Luzon Strait. Station WG2 is closer to the basin of the SCS (Figure 1) and is the deepest among the three stations (Table 1).

2.1. Experimental Design

The incubation experiments with durations of 13, 11, and 10 days, including the seawater sampling day (day 0), were conducted at station A3, station A6, and station WG2, respectively. Surface seawater (2–5 m in depth) was collected with Niskin bottles mounted on a Seabird CTD (Conductivity, Temperature, Depth, SBE 911 plus, USA). The collected water was distributed into 16 acid-cleaned 20 L Nalgene polycarbonate incubation bottles after filtering through 200 μm nylon mesh to exclude mesozooplankton. We avoided contacting trace metals by using acid-cleaned plastic or polymeric material equipment in the experiment setup and sampling processes, despite the experimental operation was not in rigorous trace metal clean environment.

The bottles were divided into eight groups (two replicates) as described in Table 2: control group, N group, P group, Fe group, N + P group, N + P + Fe group, dust group, and rainwater group. All the bottles were placed in transparent plastic vessels on the deck and bathed with running seawater pumped from sea surface to

Table 1
Nutrient Concentrations at Each Station on Day 0 of the Incubation Experiments

Station	Depth (m)	Incubation start date	NO_3^-	NO_2^-	PO_4^{3-}	SiO_3^{2-}	Chl *a*	$[NO_3^- + NO_2^-]/PO_4^{3-}$
			(μmol/L)				(μg/L)	—
A3	2,700	27 Mar	0.31	0.04	0.08	2.21	0.14	4.4
A6	3,161	12 Apr	0.55	0.04	0.02	2.67	0.14	29.5
WG2	3,963	23 Apr	0.05	0.05	0.01	2.31	0.04	10.0

maintain in situ temperature throughout the incubation (Liu et al., 2013). All bottles were gently stirred three times a day to avoid biogenic accumulation.

For dust group, 1/16 of a dust-collected filter (the dust was assumed to be uniformly collected on the filter) was placed in 20 mL Mill-Q water and extracted with ultrasonication for 1 h at 0°C (Guo et al., 2012; Hsu et al., 2010). Then, the filters and turbid solution were added to each of two incubation bottles. With above procedures, the dust added to each bottle was about 1.09 mg/L. The annual dust deposition in the SCS is estimated to be in a range of 2.5–52 g/m^2 (Gao et al., 1997; Wang et al., 2012). Assuming deposited dust was distributed evenly in the mixed layer whose depth ranges from 27 to 57 m (shallow in summer and deep in winter) (Chen & Chen, 2006), the annual dust input to surface seawater becomes approximately 0.04–1.9 mg/L. The added concentration of 1.09 mg/L in the dust group was at the middle of the annual dust deposition range.

For the rainwater group, 8 mL of rainwater was added to each of two bottles. The amount of added rainwater was under an assumption of a heavy rain event (20 mm) into a 50 m mixed layer depth.

For the elemental addition groups (N, P, and Fe added individually and in combination), the levels were selected to evaluate the limiting condition in the SCS and to identify the key element in dust affecting the marine ecosystem. The nutrients were added in concentrations based on previous incubation experiments in the SCS (Guo et al., 2012) and the Yellow Sea (Liu et al., 2013).

2.2. Dust and Rainwater Collection and Chemical Analysis

Asian dust samples were collected during the dust storm period of 9–10 March 2013. Samples were collected on Whatman 41 cellulose filters using a high volume sampler (KC-1000, Qingdao Laoshan Elec. Inc., China), placed at the Laoshan campus of Ocean University of China, Qingdao (36.10°N, 120.27°E). Our dust collection palace was in northern China, which was located in the pathways of eastward transported Asian dust, before branching southward to the SCS (Tan et al., 2012; Wang et al., 2011). During the 24 h sampling period (1.05 m^3/min), about 0.348 g of total suspended particles was collected. The filter was stored at −20°C until chemical analysis and use in incubation experiments.

To measure the dissolvable materials that leached from dust samples, a piece of the filter was placed in 20 mL Mill-Q water and extracted with ultrasonication for 1 h at 0°C (Guo et al., 2012; Hsu et al., 2010). The solution was filtered with acid-cleaned acetate cellulose filters (0.45 μm pore size) and rinsed three times with Mill-Q water. Dissolved inorganic nutrients were analyzed by Nutrient AutoAnalyzer (SEAL Analytica, AutoAnalyzer 3). For dissolved trace metals, the filtered solution was acidified and assayed by inductively coupled plasma atomic emission spectrometry (Hsu et al., 2010; Shi et al., 2012).

Rainwater (pH 4.95) was collected on 24 March 2013 during the cruise in the SCS before the incubation experiments. Acid-cleaned polyethylene bottles were placed on the upper deck of the ship for rainwater collection. The collected rainwater was stored at −20°C until chemical analysis and incubation experiments. The rainwater samples for analysis were thawed and then filtered and analyzed in the same way as the dust sample. In preparation for trace metals analysis, acidification was conducted by adding 5% ultrapure HNO_3 (Al-Momani, 2003).

Table 2
Treatment in Different Incubation Groups

Group	Treatment
Control	
N group	2 μmol/L $NaNO_3$
P group	0.2 μmol/L NaH_2PO_4
Fe group	2 nmol/L $FeSO_4$
N + P group	2 μmol/L $NaNO_3$ + 0.2 μmol/L NaH_2PO_4
N + P + Fe group	2 μmol/L $NaNO_3$ + 0.2 μmol/L NaH_2PO_4 + 2 nmol/L $FeSO_4$
Dust group	1.09 mg/L dust[a]
Rainwater group	0.4 mL/L rainwater[b]

[a]Nutrients added by dust: N, 0.57 μmol/L; P, 7.27 nmol/L; Fe, 8.67 nmol/L.
[b]Nutrients added by rainwater: N, 0.045 μmol/L; P, 0.36 nmol/L; Fe, 0.16 nmol/L.

Table 3
Dissolved Nutrients and Trace Metals in Dust and Rainwater Samples Collected Before Incubation Experiments

	Nutrients (μmol/g)					Trace metals (μg/g)									
Dust sample	NO_3^-	NO_2^-	NH_4^+	PO_4^{3-}	SiO_3^{2-}	Pb	Cr	Mn	Fe	Co	Ni	Cu	Zn	As	Cd
	166.70	5.51	355.90	6.66	1.57	32.25	29.11	3.15	445.40	2.65	31.67	100.20	281.90	21.24	0.98
	Nutrients (μmol/L)					Trace metals (μg/L)									
Rainwater sample	NO_3^-	NO_2^-	NH_4^+	PO_4^{3-}	SiO_3^{2-}	Pb	Cr	Mn	Fe	Co	Ni	Cu	Zn	As	Cd
	48.16	0.24	63.95	0.91	1.03	18.74	3.34	0.37	22.70	0.24	2.24	20.12	97.95	1.03	0.13

2.3. Sampling in the Incubation Experiments and Analysis

2.3.1. Chl *a* and Nutrients

Duplicate 300 mL (for Chl *a* concentration) and 150 mL (for nutrient concentration) samples were collected from each incubation bottle at the same time in the morning during the incubation period. The subsamples for Chl *a* measurements were filtered through acid-cleaned Whatman GF/F glass fiber filters (0.7 μm pore size). Chl *a* filters were extracted with 90% acetone at −20°C in the dark for ~24 h (Strickland & Parsons, 1972). Then the Chl *a* concentration was measured using a Turner Design Fluorometer (Turner Designs, Trilogy Laboratory Fluorometer, USA) (Guo et al., 2012).

The subsamples for dissolved inorganic nutrient concentration were filtered through acid-cleaned acetate cellulose filters (0.45 μm pore size). Then the filtrate was stored in acid-cleaned polyethylene bottles at −20°C until analysis in the laboratory. Subsamples for dissolved inorganic nutrients were analyzed by the Nutrient AutoAnalyzer (SEAL Analytica, AutoAnalyzer 3). The limit of detection for NH_4^+, NO_3^-, NO_2^-, SiO_3^{2-}, and PO_4^{3-} were 0.04, 0.02, 0.003, 0.005, and 0.01 μmol/L, respectively.

2.3.2. Phytoplankton Community Identification

A 300 mL water sample for phytoplankton community identification was collected in the morning at the same time as the Chl *a* and dissolved inorganic nutrient collection. The sampling for phytoplankton community identification was on the following schedule: days 0, 4, 8, and 12 at station A3; days 0, 4, and 8 at station A6; and days 0, 4, 7, and 9 at station WG2. Samples were immediately fixed with acidic Lugol's iodine (2% final concentration) and stored in the dark (Stibor et al., 2004). In preparation for analysis, the samples were concentrated to 10–15 mL by settling for 48 h in glass cylinders and finally examined by an inverted microscope (Nikon ECLIPSE TE2000-U) for identification of phytoplankton >5 μm in size. We took one parallel sample for the presentation of phytoplankton community, with the other parallel sample as an alternative in case the sample is broken.

3. Results

For initial seawater, slightly high DIN (0.35 μmol/L ≤ NO_3^- + NO_2^- ≤ 0.59 μmol/L) and DIP (0.02 μmol/L ≤ PO_4^{3-} ≤ 0.08 μmol/L) concentrations were observed at stations A3 and A6, compared to low concentrations (NO_3^- + NO_2^- = 0.10 μmol/L, PO_4^{3-} = 0.01 μmol/L) at station WG2 (Table 1). Other studies also reported a similar variation range of DIN (0.01–0.31 μmol/L) and DIP (0.01–0.09 μmol/L) in the spring SCS, with the ratio of N/P lower than the Redfield ratio of 16 (Chen et al., 2004; Wu et al., 2003). For the Chl *a*, which was treated as the proxy for phytoplankton biomass, we observed a variation range from 0.04 μg/L (station WG2) to 0.14 μg/L (stations A3 and A6) in our experiment (Table 1), which was comparable with the results in another study (Chen, 2005).

The dissolved inorganic nutrients and trace metals leached from the dust and rainwater are shown in Table 3. The concentration of total dissolved inorganic nitrogen (528.11 μmol N/g, including NO_3^-, NO_2^-, and NH_4^+) was relatively higher than other nutrients in both the dust and rainwater. The high N/P ratio in dust (79:1) and rainwater (123:1) implied that they supplied more nitrogen than phosphorus for phytoplankton.

3.1. Station A3

3.1.1. Chl *a* and Nutrients

Chl *a* for the N + P and N + P + Fe groups at station A3 was statistically significantly higher than that of the control group ($P_{N+P} < 0.05$, $P_{N+P+Fe} < 0.05$) with maximum values of 1.87 μg/L and 3.22 μg/L, respectively, that were 3.1-fold and 5.4-fold of the maximum Chl *a* in the control group (0.60 μg/L) (Figure 2a). The maximum value in the N group (1.60 μg/L) was 2.7-fold of the control group ($P_N < 0.01$), but the individual

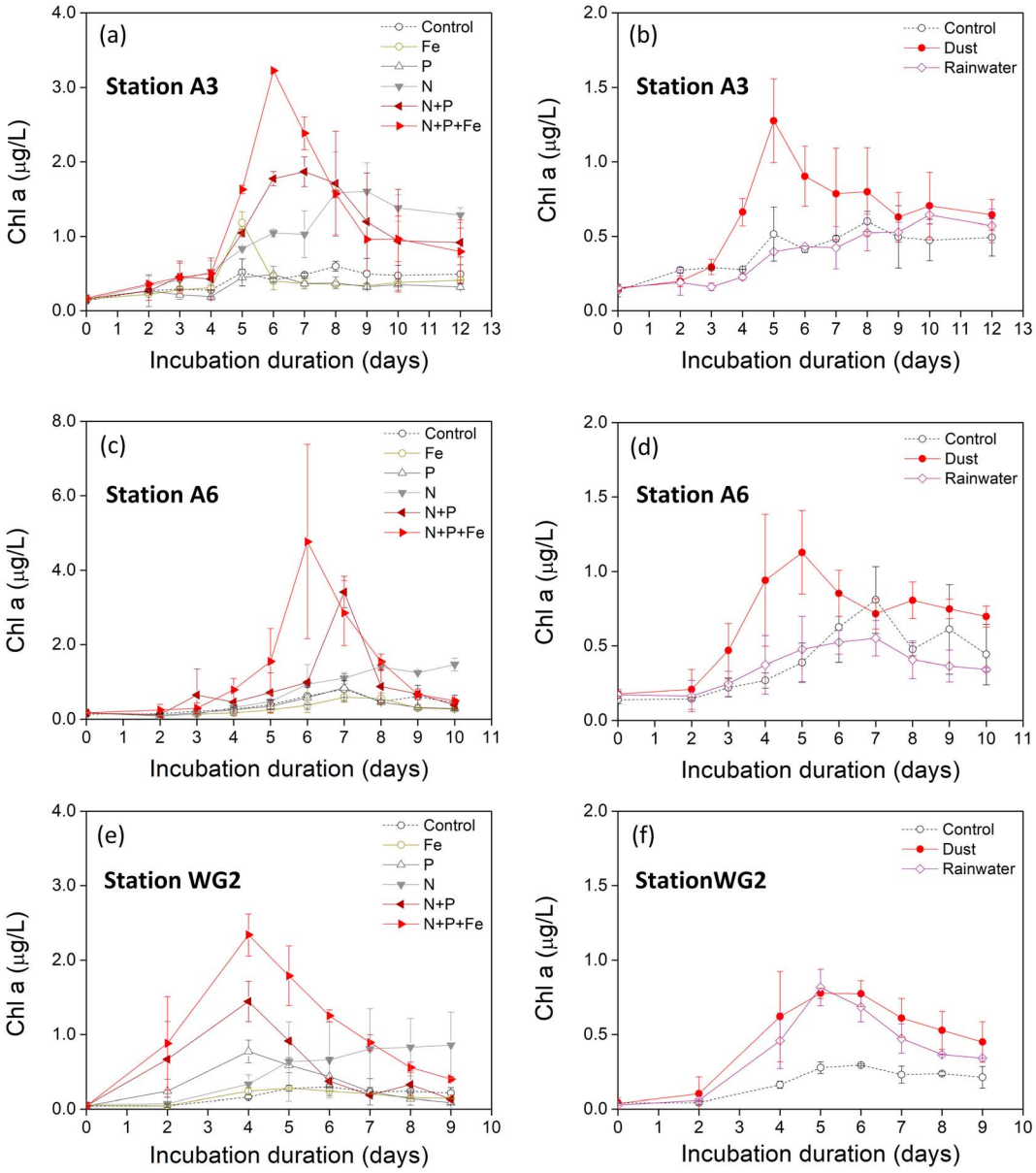

Figure 2. Measured Chl *a* concentration in nutrient addition groups (a) and dust and rainwater addition groups (b) at station A3; (c) and (d) show the same respective additions at station A6; and (e) and (f) show the same respective additions at station WG2.

addition of P or Fe did not produce an increase in Chl *a*. The maximum value in the N group occurred on day 9, which is later than the peak in the N + P group on day 7 and in the N + P and N + P + Fe groups on day 6. Both the positive response in the N and N + P groups and the negative response in the P group were consistent with previous researches in the SCS (Chen, 2005; Wu et al., 2003). The maximum Chl *a* in the dust group ($P_{dust} < 0.05$) reached 1.28 μg/L on day 5, which was about 2.1-fold of that in the control group (Figure 2b). The addition of rainwater induced no response in Chl *a*.

Consistent with the increase in Chl *a* in nitrogen-related groups, nutrient concentrations in these groups decreased. DIN decreased to 6%, 11%, and 11% of initial values in the N, N + P, and N + P + Fe groups (Figure 3) at the time of reaching the maximum Chl *a*. DIP in these groups showed a similar deceasing trend. In the rainwater group, DIN and DIP provided by rainwater was 12.9% and 0.45% of that in background seawater. Thus, DIN and DIP concentrations were low in the group during the incubation, which were similar to that in the control group. Nutrients also showed a decreasing pattern in the dust group. Interestingly, in

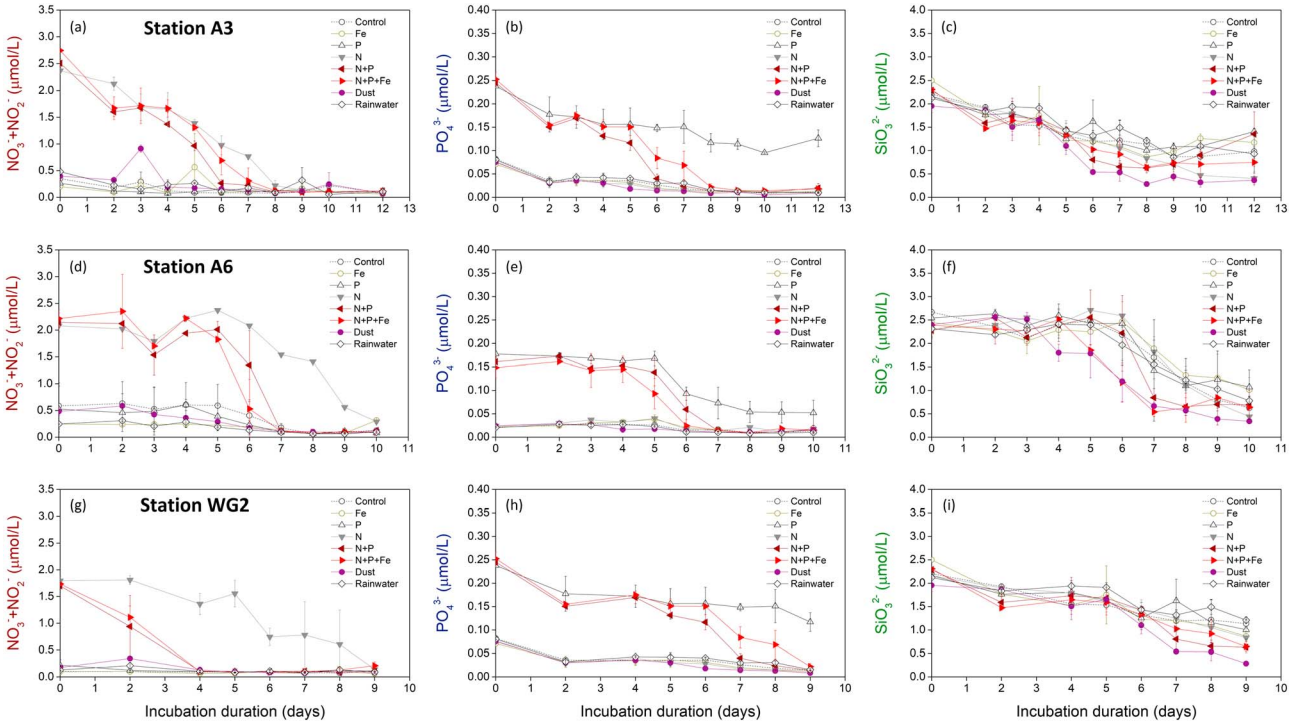

Figure 3. Measured nutrient concentrations in all incubation groups at three sites. (a)–(c) $NO_3^- + NO_2^-$, PO_4^{3-}, and SiO_3^{2-} concentrations at station A3; (d)–(f) $NO_3^- + NO_2^-$, PO_4^{3-}, and SiO_3^{2-} concentrations at station A6; (g)–(i) $NO_3^- + NO_2^-$, PO_4^{3-}, and SiO_3^{2-} concentrations at station WG2.

the N + P group, Chl *a* did not show a rapid increase in the first 4 days despite the fast decrease of nutrients. This result may reflect luxury uptake and storage of DIN and DIP by the algae (Lomas et al., 2010; Vincent, 1981). The decease of silicate in groups without an increase in Chl *a* (e.g., control and rainwater groups) also confirmed this occurrence. DIP in the N group was low during the incubation. On the contrary, Chl *a* in the N group showed an obvious increase in extremely low DIP, which indicated supplementation from other phosphorus sources. The slowly increasing trend of Chl *a* implied the slow transformation and assimilation of that phosphorus source.

3.1.2. Phytoplankton Community

In this study, 47 genera or species were recorded. Algae species from the same genera were not separately recoded. In the results, *Climacodium* spp., *Chaetoceros* spp., *Nitzschia* spp., *Leptocylindrus* spp., and *Licmophora* spp. were the dominant diatom species.

At station A3, the initial phytoplankton community (total abundance, 4.2×10^4 cells/L) was composed of diatoms, dinoflagellates, and cryptomonas with abundance percentages of 80.7%, 10.4%, and 8.9%, respectively (Table 4), and very few Chrysophyta was also recorded. The dominant species was *Climacodium* spp. with an abundance of 1.7×10^4 cells/L. The community structure showed obvious changes during the incubation. On day 4, *Chaetoceros* spp. became the dominant species in all the eight groups, especially in the N + P and N + P + Fe groups (relative abundance >80%) (Table 4). On day 8, *Chaetoceros* spp. continued to be the dominant algae in N + P and N + P + Fe groups, while in other groups, the dominant algae transitioned to different algae like *Nitzschia* spp., *Leptocylindrus* spp., or dinoflagellates. During the bloom period shown by Chl *a* concentration from days 4 to 8 in the N + P and N + P + Fe groups, the community structure showed the competitive advantage of *Chaetoceros* spp. in these groups.

3.2. Station A6

3.2.1. Chl *a* and Nutrients

The responses of Chl *a* in all incubation groups at station A6 were almost the same as those in corresponding groups at station A3 (Figures 2c and 2d). N + P and N + P + Fe groups showed an obvious Chl *a* increase with peak values of 3.42 and 4.77 μg/L, respectively, which are higher than those in other groups. Chl *a* in the

Table 4
Phytoplankton Community During Incubation Experiments at Station A3

	Day 0		Day 4		Day 8		Day 12	
Group	Dominant algae	Abundance[a] (proportion)	Dominant algae	Abundance[a] (proportion)	Dominant algae	Abundance[a] (proportion)	Dominant algae	Abundance[a] (proportion)
Control	*Climacodium* spp.	1.7 (40.7%)[b]	*Chaetoceros* spp.	5.0 (44.8%)	*Nitzschia* spp.	3.5 (37.0%)	Dinoflagellate	2.9 (36.2%)
N			*Chaetoceros* spp.	12.6 (77.6%)	*Leptocylindrus* spp.	21.2 (56.4%)	—	—
P			*Chaetoceros* spp.	7.5 (55.1%)	*Nitzschia* spp.	3.4 (38.9%)	*Nitzschia* spp.	2.4 (35.4%)
N + P			*Chaetoceros* spp.	8.5 (95.1%)	*Chaetoceros* spp.	28.9 (37.7%)	*Licmophora* spp.	55.7 (75.5%)
Dust			*Chaetoceros* spp.	8.8 (44.7%)	—	—	*Leptocylindrus* spp.	25.8 (58.2%)
Rainwater			*Chaetoceros* spp.	5.3 (70.3%)	Dinoflagellate	4.3 (48.8%)	*Leptocylindrus* spp.	8.4 (55.1%)
Fe			*Chaetoceros* spp.	5.0 (53.0%)	*Leptocylindrus* spp.	1.4 (38.1%)	*Nitzschia* spp.	2.5 (33.1%)
N + P + Fe			*Chaetoceros* spp.	33.3 (87.7%)	*Chaetoceros* spp.	13.4 (42.9%)	*Chaetoceros* spp.	5.6 (31.6%)

[a]Unit of algae abundance is 10^4 cells/L. [b]Total abundance on day 0 is 4.2×10^4 cells/L.

N + P + Fe group reached its peak 1 day earlier than in the N + P group. The N group showed a slow increase of Chl *a* that reached its highest value of 1.47 μg/L on the last day of the incubation. In the dust group, Chl *a* increased during the first 5 days and reached its peak (1.13 μg/L) even earlier than did the N + P + Fe group. The control and rainwater groups both showed similar more gradual and much smaller increases in Chl *a*.

For the nutrient additions, DIN and DIP exhibited obvious decreases in the nitrogen-related groups, especially in the N + P and N + P + Fe groups. Differing from station A3, DIN and DIP did not decrease until the Chl *a* bloom period during incubation days 4 to 8 (Figure 3). Silicate decreased in all groups at station A3, which also supported the luxury uptake of silicate in the incubation system.

3.2.2. Phytoplankton Community

At station A6, the total abundance of phytoplankton was 2.6×10^4 cells/L, which is lower than that at station A3. The composition of diatoms, dinoflagellates, and cryptomonas was 77.7%, 12.6%, and 9.7%, respectively. Although *Nitzschia* spp. was the dominant species (Table 5) at the beginning of the incubation, *Chaetoceros* spp. became dominant in all groups on days 4 and 8, and its proportion exceeded 50% in most groups. The consistency of the dominance of *Chaetoceros* spp. in N + P and N + P + Fe groups on days 4 and 8 at both stations A3 and A6 showed that *Chaetoceros* spp. was competitive in nutrient-enriched environments. These results were consistent with previous studies showing that *Chaetoceros* spp. and *Nitzschia* spp. were dominant diatoms in nutrient-enriched winter waters of the SCS (Chen, 2005). Further, the community succession for dust addition seems to be consistent with N + P and N + P + Fe addition during the bloom period.

3.3. Station WG2

3.3.1. Chl *a* and Nutrients

Surface seawater was more oligotrophic at station WG2 than at stations A3 and A6 (Table 1). Phytoplankton showed a positive response in all the groups except for the Fe group (Figures 2e and 2f). The maximum Chl *a*

Table 5
Phytoplankton Community During Incubation Experiments at Station A6

	Day 0		Day 4		Day 8	
Group	Dominant algae	Abundance[a] (proportion)	Dominant algae	Abundance[a] (proportion)	Dominant algae	Abundance[a] (proportion)
Control	*Nitzschia* spp.	2.0 (75.4%)[b]	*Chaetoceros* spp.	5.1 (69.8%)	*Chaetoceros* spp.	4.5 (75.7%)
N			*Chaetoceros* spp.	1.1 (58.7%)	*Chaetoceros* spp.	7.7 (75.9%)
P			*Chaetoceros* spp.	0.6 (53.4%)	*Chaetoceros* spp.	2.7 (57.8%)
N + P			*Chaetoceros* spp.	1.1 (54.9%)	*Chaetoceros* spp.	47.4 (51.2%)
Dust			*Chaetoceros* spp.	6.0 (54.1%)	*Chaetoceros* spp.	7.6 (68.5%)
Rainwater			*Chaetoceros* spp.	2.7 (59.7%)	*Chaetoceros* spp.	1.2 (51.3%)
Fe			*Chaetoceros* spp.	1.1 (49.9%)	*Chaetoceros* spp.	6.5 (86.1%)
N + P + Fe			*Chaetoceros* spp.	3.3 (74.5%)	*Chaetoceros* spp.	90.7 (80.7%)

[a]Unit of algae abundance is 10^4 cells/L. [b]Total abundance on day 0 is 2.6×10^4 cells/L.

Table 6
Phytoplankton Community During Incubation Experiments at Station WG2

	Day 0		Day 4		Day 7		Day 9	
Group	Dominant algae	Abundance[a] (proportion)	Dominant algae	Abundance[a] (proportion)	Dominant algae	Abundance[a] (proportion)	Dominant algae	Abundance[a] (proportion)
Control	Dinoflagellate	0.3 (69.5%)[b]	*Nitzschia* spp.	2.1 (71.1%)	*Nitzschia* spp.	4.6 (79.3%)	—	—
N			*Nitzschia* spp.	4.3 (67.4%)	*Chaetoceros* spp.	5.8 (72.0%)	*Chaetoceros* spp.	27.7 (91.5%)
P			*Nitzschia* spp.	5.8 (57.6%)	*Nitzschia* spp.	17.0 (47.9%)	*Leptocylindrus* spp.	3.2 (54.2%)
N + P			*Nitzschia* spp.	105.4 (94.5%)	Dinoflagellate	6.0 (51.0%)	*Nitzschia* spp.	3.4 (41.0%)
Dust			*Nitzschia* spp.	11.0 (96.4%)	*Nitzschia* spp.	16.4 (97.6%)	*Nitzschia* spp.	30.9 (98.3%)
Rainwater			*Nitzschia* spp.	28.9 (97.4%)	*Nitzschia* spp.	9.4 (92.1%)	*Nitzschia* spp.	8.9 (87.1%)
Fe			*Nitzschia* spp.	4.3 (68.5%)	*Nitzschia* spp.	6.5 (76.8%)	*Nitzschia* spp.	2.6 (53.7%)
N + P + Fe			*Nitzschia* spp.	64.4 (89.9%)	*Nitzschia* spp.	35.6 (87.1%)	*Nitzschia* spp.	12.2 (74.3%)

[a]Unit of algae abundance is 10^4 cells/L. [b]Total abundance on day 0 is 0.37×10^4 cells/L.

concentration in the N + P and N + P + Fe groups was 4.9-fold and 7.9-fold of that in the control group with maximum values of 1.44 and 2.34 μg/L ($P_{N+P+Fe} < 0.05$), respectively. Both of these peak values were lower than those for the N + P and N + P + Fe groups at stations A3 and A6. The Chl *a* peaks in the N + P and N + P + Fe groups both appeared on day 4, which was 2 to 3 days earlier than at the other two stations. As at stations A3 and A6, Chl *a* in the N group ($P_N < 0.05$) showed a slowly increasing pattern and reached a maximum (0.86 μg/L) on the last incubation day. In the dust group, Chl *a* ($P_{Dust} < 0.05$) showed a maximum concentration of 0.78 μg/L on day 5. However, different from the responses at stations A3 and A6, both the P and rainwater groups showed positive responses of Chl *a* with peaks of 0.77 and 0.82 μg/L, respectively, on days 4 and 5.

Nutrients at station WG2 (Figure 3) decreased markedly in the N, N + P, and N + P + Fe groups. When reaching the maximum Chl *a* during incubation, DIN concentration dropped to 8%, 6%, and 5% of the initial values in the N, N + P, and N + P + Fe groups, respectively. In the N group, DIP fluctuated at an extremely low concentration (9–15 nmol/L), which was the same as that at stations A3 and A6. DIN in P group showed a low concentration during the incubation period. Nutrients in the dust group also decreased despite having low initial values. In the rainwater group, both DIN and DIP exhibited low concentrations, while silicate showed a marked decrease from 2.2 to 0.67 μmol/L. The decrease in silicate in the control group was also the same as that observed at stations A3 and A6.

3.3.2. Phytoplankton Community

At station WG2, the phytoplankton community included diatoms and dinoflagellates with a proportion of 30.5% and 69.5%, respectively, in algae abundance (Table 6). The low total abundance of 0.37×10^4 cells/L was consistent with the low background Chl *a* concentration. After the first 4 days of incubation, *Nitzschia* spp. became the dominant species with a proportion over 50% in all eight groups. On day 4, the abundance in the N + P (105.4×10^4 cells/L) and N + P + Fe groups (64.4×10^4 cells/L) was higher than in other groups, which was also consistent with the observed higher Chl *a* peak. The dust group was not an exception with *Nitzschia* spp. being dominant during the bloom. After the bloom period, the phytoplankton communities showed slightly different succession trends in different groups, as was observed at station A3. Specifically, *Chaetoceros* spp. became the dominant species on days 7 and 9 in the N group; dinoflagellates were dominant on day 7 in the N + P group; *Leptocylindrus* spp. became dominant on day 9 in the P group. In other groups, *Nitzschia* spp. was dominant from day 4 to the end of the incubation.

4. Discussion

4.1. Nutrient Limitation in the SCS

Nutrient enrichment experiments are a well-utilized methodology for evaluating nutrient limitation in different ocean biota (Moore et al., 2013). In our in situ incubation experiments, N groups at all three stations showed a positive but slow Chl *a* response (Figure 2). However, almost all groups with the addition of phosphorus or iron alone showed no obvious Chl *a* response, which is indicative of nitrogen limitation in the SCS. Previous research also showed similar results and suggested that nitrogen plays the critical role in the SCS (Chen, 2005; Guo et al., 2012; Wu et al., 2003).

Compared to N groups, Chl *a* in N + P and N + P + Fe groups at all three stations showed faster increase and higher peaks, suggesting that phosphorus is also a limiting nutrient for the algae in nitrogen-enriched condition. Other studies also showed a more strongly positive Chl *a* response to N + P addition than to the addition of N + Si or P + Si (Guo et al., 2012). These findings were consistent with the in situ studies in the tropical Atlantic (Davey et al., 2008; Moore et al., 2008), that low-latitude surface ocean waters were universally limited by nitrogen with phosphorus being a secondary liming nutrient (Moore et al., 2013). Iron was not considered to be a strongly limiting element from our experiments as almost no Chl *a* response to the addition of iron alone was found. Chen (2005) also found no apparent Chl *a* response to the addition of iron alone by incubation experiments, although Wu et al. (2003) inferred the importance of iron on N_2 fixation process by algae. Previous research indicated that iron mostly limited the high-nutrient low-chlorophyll regions (Boyd et al., 2000; Tsuda et al., 2003) at high latitude. But for the low-nutrient low-chlorophyll regions such as the SCS, the promotion effect of iron on the ecosystem was not apparent. Overall, nitrogen and phosphorus were both urgently needed by phytoplankton in the SCS and the region was more likely to be nitrogen limited.

4.2. Phytoplankton Community Succession

In the SCS, all sized (pico-sized, nano-sized, and micro-sized) phytoplankton existed in surface seawater. With more nutrient supplementation, the abundance of micro-sized algae such as diatoms would apparently increase (Chen, 2005). In this study, we used the identification results by inverted microscope to investigate the variation of phytoplankton community during the incubation period.

Our experiments showed a similar evolution of the algae community at all three stations that diatoms became the dominant algae in apparent Chl *a*-increased groups (e.g., in N + P and N + P + Fe groups) (Tables 4–6). This dominance occurred no matter whether the dominant algae at the start of the experiments were diatoms (at stations A3 and A6) or dinoflagellates (at station WG2). These results were consistent with those of previous study that diatoms had an advantage in growth competition under nutrient-enriched conditions (Boyd et al., 2007; Chen et al., 2004; Guo et al., 2012). High growth rates of micro-sized algae coupled with low grazing pressure from zooplankton in nutrient-enriched condition was probably the reason of competitive advantage of micro-sized algae (Landry et al., 2000).

Furthermore, *Chaetoceros* spp. became the dominant diatom species during the bloom period in apparent Chl *a*-increased groups at stations A3 and A6, while *Nitzschia* spp. was the dominant diatom species at station WG2. Chen (2005) also reported that *Chaetoceros* spp. and *Nitzschia* spp. would become the dominant diatom species with more nutrient supplement in surface seawater in the SCS. After the bloom period in the incubation, the dominant algae changed to other diatom species (e.g., *Leptocylindrus* spp. or *Licmophora* spp.) or dinoflagellate (Tables 4 and 6) in most of the groups.

Changes in phytoplankton community in the presence of dust addition nearly mirrored those in N + P or N + P + Fe groups, with *Chaetoceros* spp. becoming the dominant species at stations A3 and A6, and *Nitzschia* spp. became dominant at station WG2. Other research conducted in different regions also showed similar results, such as that of showing the induction of increased abundance of diatoms by Saharan dust (Franchy et al., 2013). Some incubation studies also produced different results, such as a response from pico-sized phytoplankton for the first addition of dust, while all phytoplankton sizes show a positive response to the second addition (Giovagnetti et al., 2013). The negative response of micro-sized phytoplankton to dust addition was also reported in some studies (Herut et al., 2005).

As phytoplankton growth had a close relation with microzooplankton (e.g., nanoflagellates and ciliates) grazing in the oligotrophic SCS (Chen et al., 2009), microzooplankton could exist in our incubation systems and grew with sufficient food and less mesozooplankton control (Guo et al., 2012; Romero et al., 2011). However, the Chl *a* and algae community should not suffer much from microzooplankton grazing in the early incubation period, which is also suggested by another study (Giovagnetti et al., 2013). Another factor was bacteria that fed on dissolved organic carbon, which could also affect material flow in the incubation system. Thus, the algae community pattern after the bloom had some uncertainty under the effects of several marine organisms and biogeochemical processes.

In addition to the dominant condition in phytoplankton community during the incubation, the variation of species diversity was also estimated by using Shannon Index (Shannon & Weaver, 1949; Spellerberg &

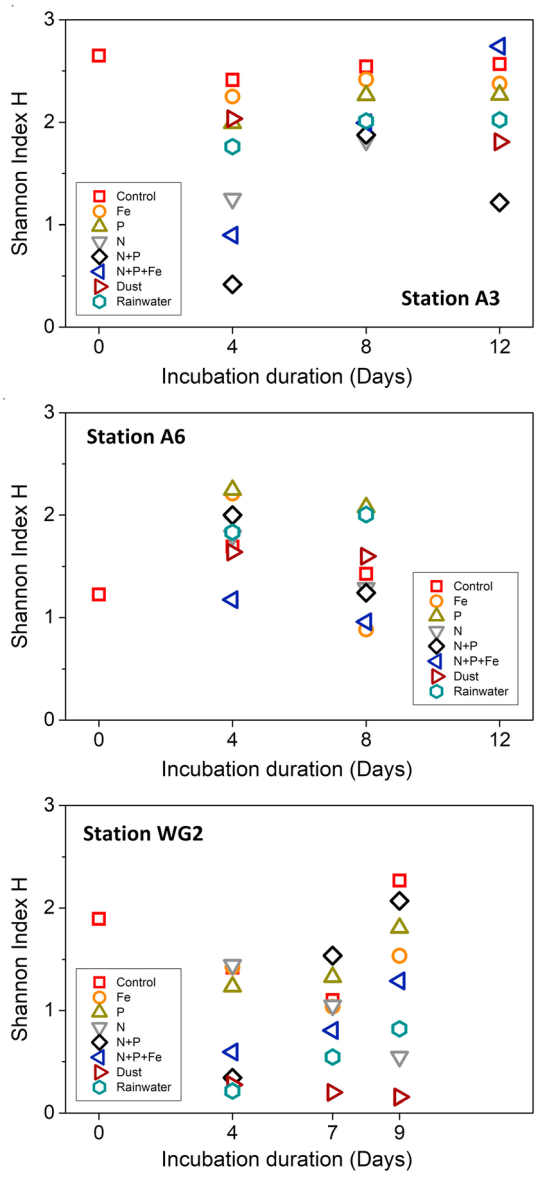

Figure 4. Shannon Index H of all incubation groups at stations A3, A6, and WG2.

Fedor, 2003) $H = -\sum_{i=1}^{S}\left(\frac{n_i}{N} \times \log_2 \frac{n_i}{N}\right)$, where n_i was the quantity of a specific species, N was the total quantity of all species, and S was species richness. From the results, lower Shannon Index values were found in the Chl *a* bloom period (~4–8 days) compared with initial values on day 0 (Figure 4). During the bloom, in apparent Chl *a* increase groups like N + P or N + P + Fe groups, the Shannon Index was generally lower than those in control groups that showed unapparent Chl *a* increase. The results indicated that species diversity would decrease when Chl *a* concentration increased. Such phenomenon was also reported in previous research in which species diversity would decrease when phytoplankton biomass reached a high level (Irigoien et al., 2004). After the bloom, the species diversity showed a slightly increasing trend indicated by higher Shannon Index in some groups on day 12 (at station A3) and day 9 (at station WG2). The dust also showed similar effect on species diversity variation with lower Shannon Index compared to control. The overall results indicated that species diversity would first decrease and then increase during the incubation experiments, in contrast to the Chl *a* variation pattern.

4.3. Possible Existence of DOP Utilization

The obvious increase of Chl *a* and the low concentration of DIP in N groups at all three stations implied another source of phosphorus assimilated by phytoplankton. The phenomenon would be clearer by the imbalance of the decreased DIP in incubation seawater and the phosphorus required by increased Chl *a*. Here a Phosphorus Requirement Index (PRI) was proposed as below:

$$\mathrm{PRI} = \frac{P_{\mathrm{required}} - P_{\mathrm{decreased}}}{P_{\mathrm{required}}}$$

$$P_{\mathrm{required}} = \Delta Chl\ a \cdot R_{c/chla} \cdot Redfield_{P/C}$$

$$P_{\mathrm{decreased}} = \Delta DIP$$

where $\Delta Chl\ a$ was the difference of Chl *a* in its peak day and 0 day, and ΔDIP was the difference of DIP in Chl *a* peak day and 0 day. We used a fixed $R_{c/chla}$ = 50 gC/(g Chl *a*) (Moll, 1998), and Redfield ratio of C/P = 106/1 in the calculation. The positive PRI value meant that the system did not supply sufficient DIP for increasing Chl *a*. The negative value meant the over supplement of DIP for Chl *a* increasing, which indicated the luxury DIP assimililation by phytoplankton during the incubation.

As presented in Figure 5, the PRI in N groups was higher than almost all the other groups, which strongly implied the presence of other undetected phosphorus sources in our experiments. The values in P groups were lowest at each station, which indicated oversupplements of DIP. Although the PRI value did not exactly reflect the accurate phosphorus demand with variable element stoichiometry in algae cells, the decreasing PRI trend in different groups and the higher values in N group still reasonably confirmed the undetected phosphorus in N groups. In addition, the Chl *a* increase in N groups showed a unique smooth increasing trend at all three stations (Figure 2), which also implied the slow assimilation of other phosphorus sources. DOP and particulate phosphorus are two possible candidates of the unknown phosphorus. However, with low remineralization rate and also low concentration of particles in the SCS (Hung et al., 2007), particulate phosphorus was not a likely possible source. On the other hand, previous research on phosphate assimilation showed that DOP was an important phosphorus source contributing to the growth of phytoplankton in oligotrophic areas (Lomas et al., 2010; Reynolds et al., 2014). Therefore, we assumed that DOP was used in the incubation experiments.

To confirm the source of phosphorus in N groups and also better realize the biological process, a biogeochemical box model with nutrients, phytoplankton, and detritus (called NPD model) (Moll, 1998; Skogen

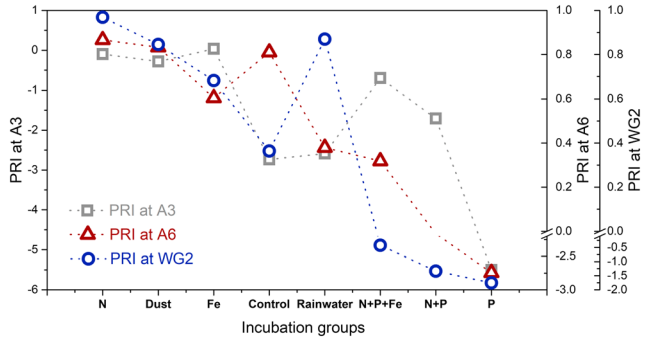

Figure 5. The Phosphorus Requirement Index (PRI) in different incubation groups at station A3 (squares), station A6 (triangles) and station WG2 (circles).

et al., 1995; Zhao & Guo, 2011) was applied to simulate our incubation experiments. The model equations and configurations are shown in Tables S1–S4 in the supporting information, and parameters referred to in previous studies (Broekhuizen et al., 1995; Chai et al., 2002; Duarte et al., 2003; Moll, 1998; Redfield, 1958; Tian et al., 2005; Zhao & Guo, 2011; Zhao et al., 2002) are shown in Table S5 in the supporting information. We found that in some groups, especially N groups, the modeled results underestimated the Chl *a* (Figure 5), mainly due to P limitation. The results also confirmed the necessity of another source of phosphorus.

To examine whether the DOP utilization can improve the model results, a simple phosphorus back-calculation scheme (shortened for PBS) based on DOP utilization mechanism was proposed. Mahaffey et al. (2014) reported that when DIP decreased below 0.03 μmol/L, DOP would be possibly used. Using 0.068 μmol/L (Table S5) as the value of DIP half-saturation constant, the limiting coefficient r_{DIP} (Table S2) would become lower than 0.3 when DIP concentration decreased below 0.03 μmol/L. Thus, when r_{DIP} was lower than 0.3 and also became the minimum of the nutrient-limiting coefficient (Table S2), we kept r_{DIP} equal to 0.3, and then DIP would be recalculated as $DIP = \frac{r_{DIP} \times K_{DIP}}{1.0 - r_{DIP}}$. The difference of DIP value before and after trigging the scheme represented the utilized DOP concentration. A up limit of DOP stock that can be used in the incubation bottle was also given in the scheme, estimated by 3.35-fold of initial DIP stock (Karl & Yanagi, 1997) in control group at each station.

After embedding the scheme, seven groups triggered the PBS (Figure 6) in the model. With PBS, the simulated Chl *a* showed a good fitting with measured values. In the three N groups, the modeled results all reproduced the slowly increasing trend of Chl *a*, despite a higher modeled peak at station A3 (Figure 6). In the two dust groups at stations A6 and WG2, the simulated Chl *a* showed a reasonable increase. However, the model did not reproduce the early appearance of the Chl *a* peak in the two dust groups. In addition, the slight increase of Chl *a* in control and rainwater groups at station A6 was also well reproduced by the model with PBS.

4.4. Promotion Effect of Dust Input in the SCS

The dust promotion effect on phytoplankton bloom has been widely reported (Giovagnetti et al., 2013; Ridame & Guieu, 2002), and the SCS was not an exception (Tan et al., 2011; Wang et al., 2012). Our incubation experiments in the region also showed a positive Chl *a* response to dust addition with the Chl *a* peak in dust groups being 2.1-fold, 1.4-fold, and 2.6-fold of those in the control incubation at stations A3, A6, and WG2 (Figure 2), respectively. The amount of phosphorus and iron that leached from the dust sample was extremely low in our experiments (Table 2). Thus, nitrogen was inferred to be the critical nutrient that promoted

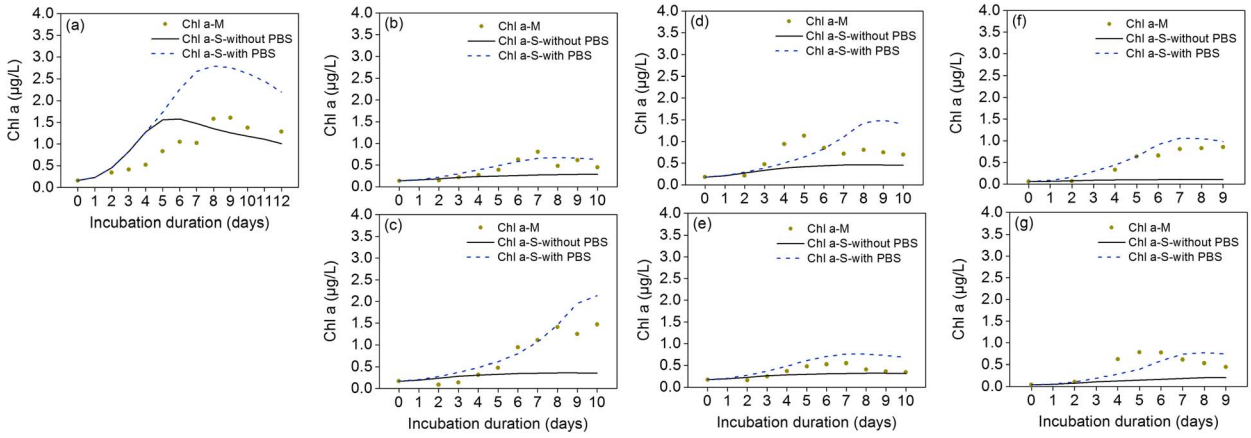

Figure 6. Measured Chl *a* (dots), simulated Chl *a* with phosphorus back-calculation scheme (PBS) (dashed lines) and without PBS (solid lines). At station A3, (a) N group; at station A6, (b) control group, (c) N group, (d) dust group and (e) rainwater group; and at station WG2, (f) N group and (g) dust group.

phytoplankton growth. The model results also showed that with the single addition of nitrogen from dust, simulated Chl *a* showed almost the same increasing trend for the addition of both nitrogen and phosphorus (Figure S1). The promotion effect in in situ experiments by Guo et al. (2012) was confirmed in our research as well, despite the fact that the aerosol in their experiment was not collected during the dust storm season.

In addition to the stimulative effect for algae blooms, the incubation experiments in the dust groups also showed a slight increase in algae growth rate, which could be known from the shorter time for Chl *a* to peak in dust groups compared to other groups at stations A3 and A6. The Chl *a* peak in dust groups appeared on day 5 of the incubation at all three stations. At stations A3 and A6, Chl *a* reached a peak on day 6 in N + P + Fe groups (Figure 2), while the peak in N + P groups was on day 7. Thus, the addition of multiple bioavailable elements by dust likely shortened the response time of Chl *a* in our experiments. These results were reasonable as trace metals were necessary for algae growth and metabolism (Wolfe-Simon et al., 2005).

Furthermore, in dust groups at stations A6 and WG2, the model with DOP utilization scheme well simulated the increase of Chl *a* but failed to reproduce the early appearance of the peak (Figure 6). The results inferred that dust might show the capacity of enhancing the transformation and assimilation of DOP, which then led to the higher growth rate of algae. Previous research also reported the importance of trace metals to alkaline phosphatase activity and then to DOP utilization (Kim & Wyckoff, 1991; McComb et al., 1979). In situ experiments also showed that trace metals like zinc could increase the alkaline phosphatase activity rate in the Atlantic Ocean (Mahaffey et al., 2014). Thus, it is reasonable to infer that trace metals in the dust could raise the growth rate by accelerating DOP transformation. As the Chl *a* peak time in the dust group at station WG2 was later than in the N + P and N + P + Fe groups, the acceleration for DOP utilization might also have an upper limit.

As our dust sampling place was located almost at the end place before Asian dust leaves the continent, the dust sample was representative of the dust deposited in the marginal seas. But during long-distance transportation, the aerosol composition could be affected by the local environment. The amounts of nutrients like particulate NO_3^- and NH_4^+ in our dust sampling place were higher than those collected in the SCS (Qi et al., 2018; Zhang et al., 2007), which was also true for trace metals, especially for Fe (Table S6). Thus, our experiments had a possibility to overestimate the promotion effect by Asian dust.

4.5. Different Responses in Oligotrophic and Ultraoligotrophic Regions

In the world ocean, oligotrophic areas are distributed mostly in the low-latitude region. Among them, some regions showed even more oligotrophic conditions, for example, at eastern Mediterranean and South Pacific gyre (Moutin et al., 2017; Thingstad et al., 2005). Although there was no specific definition to classify oligotrophic and ultraoligotrophic conditions, Moutin et al. (2012) indicated that the ultraoligotrophic regions show a deeper nitracline depth and lower primary production in the eastern Mediterranean. Thingstad et al. (2005) confirmed the ultraoligotrophic status with low surface Chl *a* concentration (0.02 μg/L) and extremely low nutrient concentration near detection limit in the eastern Mediterranean.

In our study, WG2 station possibly represented the ultraoligotrophic condition with nutrient concentrations close to detection limit and the initial Chl *a* also at a low level of 0.04 μg/L (Table 1). For the phytoplankton community, diatoms dominated the phytoplankton community at stations A3 and A6 while dinoflagellates were dominant at station WG2, which was consistent with previous research (Chen, 2005) that showed that small-sized algae dominated the community in regions with extremely low nutrients in the SCS. Previous studies indicated that the combination of the Kuroshio intrusion, ocean circulation, and eddies generated upwelling in the northern SCS (Shang et al., 2012; Shaw et al., 1996; Xiu & Chai, 2011). Since our sampling stations were near an upwelling center located about 100 km northwest off Luzon Island (Liu et al., 2002), the slightly higher nutrients and Chl *a* at stations A3 and A6 might be due to the upwelling.

In ultraoligotrophic environment, the Chl *a* response showed different characters in some incubation groups at station WG2, compared to those at stations A3 and A6. At station WG2, the incubation system exhibited a faster phytoplankton growth in response to both nitrogen- and phosphorus-enriched environment, indicated by the earlier appearance of the Chl *a* peak in N + P and N + P + Fe groups (on day 4) than corresponding groups (on day 6 or 7) at stations A3 and A6. Also, in the modeling, a higher maximum growth rate (Table S5) was needed when simulating the incubations at station WG2 in order to reproduce the early appearance of Chl *a* peaks.

Interestingly, the single addition of phosphorus promoted extra phytoplankton growth only at station WG2 (Figure 2). Under extremely low nitrogen concentration (0.1 μmol/L) in background seawaters at station WG2, the Chl *a* in P group at station WG2 suggested that phytoplankton communities might have initiated some mechanisms to relieve the stress of depleted DIN. And previous research also reported the existence and importance of N_2 fixation processes in the SCS (Chen, 2005; Chen et al., 2014; Wu et al., 2003). As the incubation seawater was filtered through nylon mesh at the beginning of the experiments, the N_2 fixation conducted by diazotroph *Trichodesmium* spp. which always gathered in clusters might be weakened. And at station WG2, N_2 fixation might be mainly conducted by unicellular diazotrophs, which was reported dominating the N_2 fixation process in ultraoligotrophic regions (Moutin et al., 2017). For the P group at station WG2, since N_2 fixation was easily constrained by availability of DIP or Fe, or both (Capone, 2001; Mills et al., 2004; Sanudo-Wilhelmy et al., 2001), the abundant phosphate in the P group might lead to the promotion of N_2 fixation processes and further lead to Chl *a* increase.

Rainwater deposition is an important input of multiple nutrients and trace metals to the ocean (Duce et al., 1991; Jung et al., 2013), though in situ researches were scarce. In a previous study in the SCS, Cui et al. (2016) reported the slightly positive Chl *a* response to rainwater deposition in incubation experiments. From our experiment, the response in the rainwater groups was different in the two different regions in the SCS. The Chl *a* responses were slight at stations A3 and A6, compared with the apparent positive response at station WG2. The slight response possibly resulted from assimilation of background nutrients at stations A3 and A6, as the Chl *a* in control groups also showed a similar slight increase at the two stations. But at station WG2, DOP utilization and N_2 fixation might both exist, which contributed to the Chl *a* increase in the rainwater group. Trace metals in the rainwater might have strengthened the two processes leading to the more apparent Chl *a* increase over that of the control at station WG2.

5. Conclusion

To evaluate marine ecosystem responses to atmospheric forcing, especially dust deposition in the SCS, we conducted onboard incubation experiments with surface seawater sampled at three stations. The entire process including bloom and recession were shown in the different incubation groups with nutrients (nitrogen, phosphorus, and iron), dust, and rainwater additions. At all three stations, the addition of nitrogen alone, rather than addition of phosphorus or iron alone, showed a stimulatory effect on phytoplankton growth, indicating that nitrogen is the most critical nutrient in the SCS. Since the N + P and N + P + Fe groups showed an even higher Chl *a* peak than the N group, phosphorus could be the secondary limiting nutrient. Under such nutrient condition in the SCS, dust showed an apparent promotion effect on phytoplankton growth by providing sufficient nitrogen. The early appearance of the Chl *a* peak in dust groups also indicated the ability of increasing algae growth rate by dust, probably due to trace metals leaching from the dust.

During the incubation, the ecosystem showed a succession in phytoplankton community. The initial ecosystem was dominated by either diatoms or dinoflagellates, and diatoms became the dominant algae during the bloom period in nutrient-enriched environments (e.g., in N + P, N + P + Fe, and dust groups). *Nitzschia* spp. and *Chaetoceros* spp. were the dominant species of diatoms. The community succession showed no apparent difference between dust group and N + P as well as N + P + Fe groups. Our results indicated the possibility that the algae community would change under external nutrient addition.

In our incubation experiments, N groups at all three stations showed a positive response and slowly increasing trend of Chl *a* in the condition of DIP deficiency. The high PRI values in N groups confirmed the undetected source of phosphorus. Also, from model perspective, after embedding a PBS scheme, the model results can better reproduce the Chl *a* increasing pattern in N groups and also some other groups. From both experimental and model perspectives, we proposed the possible existence of DOP utilization by the algae in the SCS.

In addition, different initial condition in background seawater indicated the possible presence of oligotrophic (stations A3 and A6) and ultraoligotrophic (station WG2) regions in the SCS. At the ultraoligotrophic station WG2, Chl *a* and nutrient concentrations were extremely low, while Chl *a* showed faster response to abundant nutrient addition (e.g., N + P and N + P + Fe groups) with a higher algae growth rate. The dominant algae at station WG2 changed from dinoflagellates to diatoms, and *Nitzschia* spp. was the dominant diatom species

during the bloom period. On the other hand, the dominant algae at stations A3 and A6 were always diatoms in which *Chaetoceros* spp. was dominant. The positive response of Chl *a* in the P group at station WG2 implied that other bioavailable nitrogen sources might exist, for example, N_2 fixation, since the background DIN in the seawater was scarce. Rainwater groups at station WG2 also showed a positive Chl *a* response, but those at stations A3 and A6 did not. As rainwater provided little added nutrients, N_2 fixation and DOP utilization processes might both have contributed to the algae growth.

Acknowledgments
The authors gratefully acknowledge Jinhui Shi and Xiaohuan Liu at Ocean University of China for their help in the incubation experiments and Yan Li at First Institute of Oceanography for the help in phytoplankton community identification. This work is funded by the National Nature Science Foundation of China (41210008), the National Key Basic Research Program of China (2014CB953700) and the NSFC-Shandong Joint Fund for Marine Ecology and Environmental Sciences (U1606404). Qiang Chu thanks the China Scholarship Council (CSC) for supporting his stay in Japan. Xinyu Guo thanks support of the Fundamental Research Funds for Central Universities of the Ministry of Education of China under the contract 201512004. Huiwang Gao is thankful for the support by the Ministry of Education, Culture, Sports, Science and Technology, Japan (MEXT) to a project on Joint Usage/Research Center-Leading Academia in Marine and Environment Pollution Research (LaMer). The data used in this study are provided in the files in the supporting information and also available upon request to the corresponding author.

References

Al-Momani, I. F. (2003). Trace elements in atmospheric precipitation at Northern Jordan measured by ICP-MS: Acidity and possible sources. *Atmospheric Environment*, *37*(32), 4507–4515. https://doi.org/10.1016/S1352-2310(03)00562-4

Arrigo, K. R. (2005). Marine microorganisms and global nutrient cycles. *Nature*, *437*(7057), 349–355. https://doi.org/10.1038/nature04159

Boyd, P. W., Watson, A. J., Law, C. S., & Abraham, E. R. (2000). A mesoscale phytoplankton bloom in the polar Southern Ocean stimulated by iron fertilization. *Nature*, *407*(6805), 695–702. https://doi.org/10.1038/35037500

Boyd, P. W., Jickells, T., Law, C. S., Blain, S., Boyle, E. A., Buesseler, K. O., et al. (2007). Mesoscale iron enrichment experiments 1993–2005: Synthesis and future directions. *Science*, *315*(5812), 612–617. https://doi.org/10.1126/science.1131669

Broekhuizen, N., Heath, M. R., Hay, S. J., & Gurney, W. S. C. (1995). Modelling the dynamics of the North Sea's mesozooplankton. *Netherlands Journal of Sea Research*, *33*(3-4), 381–406. https://doi.org/10.1016/0077-7579(95)90054-3

Capone, D. G. (2001). Marine nitrogen fixation: What's the fuss? *Current Opinion in Microbiology*, *4*(3), 341–348. https://doi.org/10.1016/S1369-5274(00)00215-0

Chai, F., Dugdale, R. C., Peng, T. H., Wilkerson, F. P., & Barber, R. T. (2002). One-dimensional ecosystem model of the equatorial Pacific upwelling system. Part I: Model development and silicon and nitrogen cycle. *Deep Sea Research Part II: Topical Studies in Oceanography*, *49*(13-14), 2713–2745. https://doi.org/10.1016/S0967-0645(02)00055-3

Chen, Y.-L. L. (2005). Spatial and seasonal variations of nitrate-based new production and primary production in the South China Sea. *Deep Sea Research Part I: Oceanographic Research Papers*, *52*(2), 319–340. https://doi.org/10.1016/j.dsr.2004.11.001

Chen, Y.-L. L., & Chen, H.-Y. (2006). Seasonal dynamics of primary and new production in the northern South China Sea: The significance of river discharge and nutrient advection. *Deep Sea Research Part I: Oceanographic Research Papers*, *53*(6), 971–986. https://doi.org/10.1016/j.dsr.2006.02.005

Chen, Y.-L. L., Chen, H.-Y., Karl, D. M., & Takahashi, M. (2004). Nitrogen modulates phytoplankton growth in spring in the South China Sea. *Continental Shelf Research*, *24*(4-5), 527–541. https://doi.org/10.1016/j.csr.2003.12.006

Chen, B., Liu, H., Landry, M. R., Dal, M., Huang, B., & Sune, J. (2009). Close coupling between phytoplankton growth and microzooplankton grazing in the western South China Sea. *Limnology and Oceanography*, *54*(4), 1084–1097. https://doi.org/10.4319/lo.2009.54.4.1084

Chen, Y.-L. L., Chen, H.-Y., Lin, Y.-H., Yong, T.-C., Taniuchi, Y., & Tuo, S.-h. (2014). The relative contributions of unicellular and filamentous diazotrophs to N_2 fixation in the South China Sea and the upstream Kuroshio. *Deep Sea Research Part I: Oceanographic Research Papers*, *85*, 56–71. https://doi.org/10.1016/j.dsr.2013.11.006

Cui, D.-Y., Wang, J.-T., Tan, L.-J., & Dong, Z.-Y. (2016). Impact of atmospheric wet deposition on phytoplankton community structure in the South China Sea. *Estuarine, Coastal and Shelf Science*, *173*, 1–8. https://doi.org/10.1016/j.ecss.2016.02.011

Davey, M., Tarran, G. A., Mills, M. M., Ridame, C., Geider, R. J., & LaRoche, J. (2008). Nutrient limitation of picophytoplankton photosynthesis and growth in the tropical North Atlantic. *Limnology and Oceanography*, *53*(5), 1722–1733. https://doi.org/10.4319/lo.2008.53.5.1722

Duarte, P., Meneses, R., Hawkins, A. J. S., Zhu, M., Fang, J., & Grant, J. (2003). Mathematical modelling to assess the carrying capacity for multi-species culture within coastal waters. *Ecological Modelling*, *168*(1-2), 109–143. https://doi.org/10.1016/S0304-3800(03)00205-9

Duce, R. A., Liss, P. S., Merrill, J. T., Atlas, E. L., Buat-Menard, P., Hicks, B. B., et al. (1991). The atmospheric input of trace species to the world ocean. *Global Biogeochemical Cycles*, *5*(3), 193–259. https://doi.org/10.1029/91GB01778

Duce, R. A., LaRoche, J., Altieri, K., Arrigo, K. R., Baker, A. R., Capone, D. G., et al. (2008). Impacts of atmospheric anthropogenic nitrogen on the open ocean. *Science*, *320*(5878), 893–897. https://doi.org/10.1126/science.1150369

Eppley, R. W., & Peterson, B. J. (1979). Particulate organic matter flux and planktonic new production in the deep ocean. *Nature*, *282*(5740), 677–680. https://doi.org/10.1038/282677a0

Franchy, G., Ojeda, A., López-Cancio, J., & Hernández-León, S. (2013). Plankton community response to Saharan dust fertilization in subtropical waters off the Canary Islands. *Biogeosciences Discussions*, *10*(11), 17,275–17,307. https://doi.org/10.5194/bgd-10-17275-2013

Gao, Y., Arimoto, R., Duce, R. A., Zhang, X.-Y., Zhang, G.-Y., An, Z.-S., et al. (1997). Temporal and spatial distributions of dust and its deposition to the China Sea. *Tellus Series B: Chemical and Physical Meteorology*, *49*(2), 172–189. https://doi.org/10.3402/tellusb.v49i2.15960

Giovagnetti, V., Brunet, C., Conversano, F., Tramontano, F., Obernosterer, I., Ridame, C., & Guieu, C. (2013). Assessing the role of dust deposition on phytoplankton ecophysiology and succession in a low-nutrient low-chlorophyll ecosystem: A mesocosm experiment in the Mediterranean Sea. *Biogeosciences*, *10*(5), 2973–2991. https://doi.org/10.5194/bg-10-2973-2013

Guo, C., Yu, J., Ho, T. Y., Wang, L., Song, S., Kong, L., & Liu, H. (2012). Dynamics of phytoplankton community structure in the South China Sea in response to the east Asian aerosol input. *Biogeosciences*, *9*(4), 1519–1536. https://doi.org/10.5194/bg-9-1519-2012

Herbland, A., Le Bouteiller, A., & Raimbault, P. (1985). Size structure of phytoplankton biomass in the equatorial Atlantic Ocean. *Deep Sea Research Part A: Oceanographic Research Papers*, *32*(7), 819–836. https://doi.org/10.1016/0198-0149(85)90118-9

Herut, B., Zohary, T., Krom, M. D., Mantoura, R. F. C., Pitta, P., Psarra, S., et al. (2005). Response of East Mediterranean surface water to Saharan dust: On-board microcosm experiment and field observations. *Deep Sea Research Part II: Topical Studies in Oceanography*, *52*(22-23), 3024–3040. https://doi.org/10.1016/j.dsr2.2005.09.003

Hsu, S.-C., Wong, G. T. F., Gong, G. C., Shiah, F. K., Huang, Y. T., Kao, S. J., et al. (2010). Sources, solubility, and dry deposition of aerosol trace elements over the East China Sea. *Marine Chemistry*, *120*(1-4), 116–127. https://doi.org/10.1016/j.marchem.2008.10.003

Hung, J.-J., Wang, S.-M., & Chen, Y.-L. (2007). Biogeochemical controls on distributions and fluxes of dissolved and particulate organic carbon in the northern South China Sea. *Deep Sea Research Part II: Topical Studies in Oceanography*, *54*(14-15), 1486–1503. https://doi.org/10.1016/j.dsr2.2007.05.006

Irigoien, X., Huisman, J., & Harris, R. P. (2004). Global biodiversity patterns of marine phytoplankton and zooplankton. *Nature*, *429*(6994), 863–867. https://doi.org/10.1038/nature02593

Jickells, T. D., An, Z. S., Andersen, K. K., Baker, A. R., Bergametti, G., Brooks, N., et al. (2005). Global iron connections between desert dust, ocean biogeochemistry, and climate. *Science*, *308*(5718), 67–71. https://doi.org/10.1126/science.1105959

Jung, J., Furutani, H., Uematsu, M., Kim, S., & Yoon, S. (2013). Atmospheric inorganic nitrogen input via dry, wet, and sea fog deposition to the subarctic western North Pacific Ocean. *Atmospheric Chemistry and Physics*, *13*(1), 411–428. https://doi.org/10.5194/acp-13-411-2013

Karl, D. M., & Yanagi, K. (1997). Partial characterization of the dissolved organic phosphorus pool in the oligotrophic North Pacific Ocean. *Limnology and Oceanography*, *42*(6), 1398–1405. https://doi.org/10.4319/lo.1997.42.6.1398

Kim, E. E., & Wyckoff, H. W. (1991). Reaction mechanism of alkaline phosphatase based on crystal structures. *Journal of Molecular Biology*, *218*(2), 449–464. https://doi.org/10.1016/0022-2836(91)90724-K

Landry, M. R., Constantinou, J., Latasa, M., Brown, S. L., Bidigare, R. R., & Ondrusek, M. E. (2000). Biological response to iron fertilization in the eastern equatorial Pacific (IronEx II). III. Dynamics of phytoplankton growth and microzooplankton grazing. *Marine Ecology Progress Series*, *201*, 57–72. https://doi.org/10.3354/meps201057

Lin, X., Zhang, H., Huang, B.-Q., & Lin, S.-J. (2012). Alkaline phosphatase gene sequence characteristics and transcriptional regulation by phosphate limitation in *Karenia brevis* (Dinophyceae). *Harmful Algae*, *17*, 14–24. https://doi.org/10.1016/j.hal.2012.02.005

Liu, K.-K., Chao, S.-Y., Shaw, P.-T., Gong, G.-C., Chen, C.-C., & Tang, T.-Y. (2002). Monsoon-forced chlorophyll distribution and primary production in the South China Sea: Observations and a numerical study. *Deep Sea Research Part I: Oceanographic Research Papers*, *49*(8), 1387–1412. https://doi.org/10.1016/S0967-0637(02)00035-3

Liu, Y., Zhang, T.-R., Shi, J.-H., Gao, H.-W., & Yao, X.-H. (2013). Responses of chlorophyll a to added nutrients, Asian dust, and rainwater in an oligotrophic zone of the Yellow Sea: Implications for promotion and inhibition effects in an incubation experiment. *Journal of Geophysical Research: Biogeosciences*, *118*, 1763–1772. https://doi.org/10.1002/2013JG002329

Lomas, M. W., Burke, A. L., Lomas, D. A., Bell, D. W., Shen, C., Dyhrman, S. T., & Ammerman, J. W. (2010). Sargasso Sea phosphorus biogeochemistry: An important role for dissolved organic phosphorus (DOP). *Biogeosciences*, *7*(2), 695–710. https://doi.org/10.5194/bg-7-695-2010

Mahaffey, C., Reynolds, S., Davis, C. E., & Lohan, M. C. (2014). Alkaline phosphatase activity in the subtropical ocean: Insights from nutrient, dust and trace metal addition experiments. *Frontiers in Marine Science*, *1*(73), 1–13. https://doi.org/10.3389/fmars.2014.00073

McComb, R. B., Bowers, G. N. Jr., & Posen, S. (1979). *Alkaline phosphatase*. New York: Plenum Press. https://doi.org/10.1007/978-1-4613-2970-1

Mills, M. M., Ridame, C., Davey, M., La Roche, J., & Geider, R. J. (2004). Iron and phosphorus co-limit nitrogen fixation in the eastern tropical North Atlantic. *Nature*, *429*(6989), 292–294. https://doi.org/10.1038/nature02550

Moll, A. (1998). Regional distribution of primary production in the North Sea simulated by a three-dimensional model. *Journal of Marine Systems*, *16*(1-2), 151–170. https://doi.org/10.1016/S0924-7963(97)00104-8

Moore, C. M., Mills, M. M., Langlois, R., Milne, A., Achterberg, E. P., La Roche, J., & Geider, R. J. (2008). Relative influence of nitrogen and phosphorous availability on phytoplankton physiology and productivity in the oligotrophic sub-tropical North Atlantic Ocean. *Limnology and Oceanography*, *53*(1), 291–305. https://doi.org/10.4319/lo.2008.53.1.0291

Moore, C. M., Mills, M., Arrigo, K., Berman-Frank, I., Bopp, L., Boyd, P., et al. (2013). Processes and patterns of oceanic nutrient limitation. *Nature Geoscience*, *6*(9), 701–710. https://doi.org/10.1038/ngeo1765

Moutin, T., Van Wambeke, F., & Prieur, L. (2012). Introduction to the Biogeochemistry from the Oligotrophic to the Ultraoligotrophic Mediterranean (BOUM) experiment. *Biogeosciences*, *9*(10), 3817–3825. https://doi.org/10.5194/bg-9-3817-2012

Moutin, T., Doglioli, A. M., de Verneil, A., & Bonnet, S. (2017). Preface: The Oligotrophy to the UlTra-oligotrophy PACific Experiment (OUTPACE cruise, 18 February to 3 April 2015). *Biogeosciences*, *14*(13), 3207–3220. https://doi.org/10.5194/bg-14-3207-2017

Qi, J., Liu, X., Yao, X., Zhang, R., Chen, X., Lin, X., et al. (2018). The concentration, source and deposition flux of ammonium and nitrate in atmospheric particles during dust events at a coastal site in northern China. *Atmospheric Chemistry and Physics*, *18*(2), 571–586. https://doi.org/10.5194/acp-18-571-2018

Redfield, A. C. (1958). The biological control of chemical factors in the environment. *American Scientist*, *46*(3), 230A–221A.

Reynolds, S., Mahaffey, C., Roussenov, V., & Williams, R. G. (2014). Evidence for production and lateral transport of dissolved organic phosphorus in the eastern subtropical North Atlantic. *Global Biogeochemical Cycles*, *28*, 805–824. https://doi.org/10.1002/2013GB004801

Ridame, C., & Guieu, C. (2002). Saharan input of phosphate to the oligotrophic water of the open western Mediterranean Sea. *Limnology and Oceanography*, *47*(3), 856–869. https://doi.org/10.4319/lo.2002.47.3.0856

Ridame, C., Dekaezemacker, J., Guieu, C., Bonnet, S., L'Helguen, S., & Malien, F. (2014). Contrasted Saharan dust events in LNLC environments: Impact on nutrient dynamics and primary production. *Biogeosciences*, *11*(17), 4783–4800. https://doi.org/10.5194/bg-11-4783-2014

Romero, E., Peters, F., Marrasé, C., Guadayol, Ò., Gasol, J. M., & Weinbauer, M. G. (2011). Coastal Mediterranean plankton stimulation dynamics through a dust storm event: An experimental simulation. *Estuarine, Coastal and Shelf Science*, *93*(1), 27–39. https://doi.org/10.1016/j.ecss.2011.03.019

Sanudo-Wilhelmy, S. A., Kustka, A. B., Gobler, C. J., Hutchins, D. A., Yang, M., Lwiza, K., et al. (2001). Phosphorus limitation of nitrogen fixation by *Trichodesmium* in the central Atlantic Ocean. *Nature*, *411*(6833), 66–69. https://doi.org/10.1038/35075041

Shang, S.-L., Li, L., Li, J., Li, Y.-H., Lin, G., & Sun, J. (2012). Phytoplankton bloom during the northeast monsoon in the Luzon Strait bordering the Kuroshio. *Remote Sensing of Environment*, *124*, 38–48. https://doi.org/10.1016/j.rse.2012.04.022

Shannon, C. E., & Weaver, W. (1949). The mathematical theory of information.

Shao, Y.-P., Wyrwoll, K.-H., Chappell, A., Huang, J.-P., Lin, Z.-H., McTainsh, G. H., et al. (2011). Dust cycle: An emerging core theme in Earth system science. *Aeolian Research*, *2*(4), 181–204. https://doi.org/10.1016/j.aeolia.2011.02.001

Shaw, P.-T., Chao, S.-Y., Liu, K.-K., Pai, S.-C., & Liu, C.-T. (1996). Winter upwelling off Luzon in the northeastern South China Sea. *Journal of Geophysical Research*, *101*(C7), 16,435–16,448. https://doi.org/10.1029/96JC01064

Shi, J.-H., Gao, H.-W., Zhang, J., Tan, S.-C., Ren, J.-L., Liu, C.-G., et al. (2012). Examination of causative link between a spring bloom and dry/wet deposition of Asian dust in the Yellow Sea, China. *Journal of Geophysical Research*, *117*, D17304. https://doi.org/10.1029/2012JD017983

Skogen, M. D., Svendsen, E., Berntsen, J., Aksnes, D., & Ulvestad, K. B. (1995). Modelling the primary production in the North Sea using a coupled three-dimensional physical-chemical-biological ocean model. *Estuarine, Coastal and Shelf Science*, *41*(5), 545–565. https://doi.org/10.1016/0272-7714(95)90026-8

Spellerberg, I. F., & Fedor, P. J. (2003). A tribute to Claude Shannon (1916–2001) and a plea for more rigorous use of species richness, species diversity and the 'Shannon-Wiener' index. *Global Ecology and Biogeography*, *12*(3), 177–179. https://doi.org/10.1046/j.1466-822X.2003.00015.x

Stibor, H., Vadstein, O., Diehl, S., Gelzleichter, A., Hansen, T., Hantzsche, F., et al. (2004). Copepods act as a switch between alternative trophic cascades in marine pelagic food webs. *Ecology Letters*, *7*(4), 321–328. https://doi.org/10.1111/j.1461-0248.2004.00580.x

Strickland, J. D., & Parsons, T. R. (1972). A practical handbook of seawater analysis. *Bulletin of Fisheries Research Board of Canada*, *167*, 201–213.

Tan, S.-C., Shi, G.-Y., Shi, J.-H., Gao, H.-W., & Yao, X. (2011). Correlation of Asian dust with chlorophyll and primary productivity in the coastal seas of China during the period from 1998 to 2008. *Journal of Geophysical Research*, *116*, G02029. https://doi.org/10.1029/2010JG001456

Tan, S.-C., Shi, G.-Y., & Wang, H. (2012). Long-range transport of spring dust storms in Inner Mongolia and impact on the China seas. *Atmospheric Environment*, *46*, 299–308. https://doi.org/10.1016/j.atmosenv.2011.09.058

Thingstad, T. F., Krom, M. D., Mantoura, R. F., Flaten, G. A., Groom, S., Herut, B., et al. (2005). Nature of phosphorus limitation in the ultraoligotrophic eastern Mediterranean. *Science*, *309*(5737), 1068–1071. https://doi.org/10.1126/science.1112632

Thingstad, T. F., Havskum, H., Zweifel, U. L., Berdalet, E., Sala, M. M., Peters, F., et al. (2007). Ability of a "minimum" microbial food web model to reproduce response patterns observed in mesocosms manipulated with N and P, glucose, and Si. *Journal of Marine Systems*, *64*(1-4), 15–34. https://doi.org/10.1016/j.jmarsys.2006.02.009

Tian, T., Wei, H., Su, J., & Chung, C. (2005). Simulations of annual cycle of phytoplankton production and the utilization of nitrogen in the Yellow Sea. *Journal of Oceanography*, *61*(2), 343–357. https://doi.org/10.1007/s10872-005-0045-z

Tsuda, A., Takeda, S., Saito, H., Nishioka, J., Nojiri, Y., Kudo, I., et al. (2003). A mesoscale iron enrichment in the western subarctic Pacific induces a large centric diatom bloom. *Science*, *300*(5621), 958–961. https://doi.org/10.1126/science.1082000

Van den Meersche, K., Middelburg, J. J., Soetaert, K., van Rijswijk, P., Boschker, H. T. S., & Heip, C. H. R. (2004). Carbon-nitrogen coupling and algal-bacterial interactions during an experimental bloom: Modeling a ^{13}C tracer experiment. *Limnology and Oceanography*, *49*(3), 862–878. https://doi.org/10.4319/lo.2004.49.3.0862

Vincent, W. F. (1981). Rapid physiological assays for nutrient demand by the plankton. I. Nitrogen. *Journal of Plankton Research*, *3*(4), 685–697. https://doi.org/10.1093/plankt/3.4.685

Vitousek, P. M., & Howarth, R. W. (1991). Nitrogen limitation on land and in the sea: How can it occur? *Biogeochemistry*, *13*(2), 87–115. https://doi.org/10.1007/bf00002772

Wang, S.-H., Tsay, S. C., Lin, N. H., Hsu, N. C., Bell, S. W., Li, C., et al. (2011). First detailed observations of long-range transported dust over the northern South China Sea. *Atmospheric Environment*, *45*(27), 4804–4808. https://doi.org/10.1016/j.atmosenv.2011.04.077

Wang, S.-H., Hsu, N. C., Tsay, S.-C., Lin, N.-H., Sayer, A. M., Huang, S.-J., & Lau, W. K. M. (2012). Can Asian dust trigger phytoplankton blooms in the oligotrophic northern South China Sea? *Geophysical Research Letters*, *39*, L05811. https://doi.org/10.1029/2011GL050415

Wolfe-Simon, F., Grzebyk, D., Schofield, O., & Falkowski, P. G. (2005). The role and evolution of superoxide dismutases in algae. *Journal of Phycology*, *41*(3), 453–465. https://doi.org/10.1111/j.1529-8817.2005.00086.x

Wong, G. T. F., Ku, T.-L., Mulholland, M., Tseng, C.-M., & Wang, D.-P. (2007). The SouthEast Asian Time-series Study (SEATS) and the biogeochemistry of the South China Sea—An overview. *Deep Sea Research Part II: Topical Studies in Oceanography*, *54*(14-15), 1434–1447. https://doi.org/10.1016/j.dsr2.2007.05.012

Wu, J.-F., Chung, S.-W., Wen, L.-S., Liu, K.-K., Chen, Y.-L. L., Chen, H.-Y., & Karl, D. M. (2003). Dissolved inorganic phosphorus, dissolved iron, and *Trichodesmium* in the oligotrophic South China Sea. *Global Biogeochemical Cycles*, *17*(1), 1008. https://doi.org/10.1029/2002GB001924

Xiu, P., & Chai, F. (2011). Modeled biogeochemical responses to mesoscale eddies in the South China Sea. *Journal of Geophysical Research*, *116*, C10006. https://doi.org/10.1029/2010JC006800

Yuan, W., & Zhang, J. (2006). High correlations between Asian dust events and biological productivity in the western North Pacific. *Geophysical Research Letters*, *33*, L07603. https://doi.org/10.1029/2005GL025174

Zhang, Y., Sperber, K. R., & Boyle, J. S. (1997). Climatology and interannual variation of the East Asian winter monsoon: Results from the 1979–95 NCEP/NCAR reanalysis. *Monthly Weather Review*, *125*(10), 2605–2619. https://doi.org/10.1175/1520-0493(1997)125%3C2605:caivot%3E2.0.co;2

Zhang, X. Y., Zhuang, G. S., Guo, J. H., Yin, K. D., & Zhang, P. (2007). Characterization of aerosol over the northern South China Sea during two cruises in 2003. *Atmospheric Environment*, *41*(36), 7821–7836. https://doi.org/10.1016/j.atmosenv.2007.06.031

Zhao, L., & Guo, X.-Y. (2011). Influence of cross-shelf water transport on nutrients and phytoplankton in the East China Sea: A model study. *Ocean Science*, *7*(1), 27–43. https://doi.org/10.5194/os-7-27-2011

Zhao, L., Wei, H., & Feng, S.-Z. (2002). Annual cycle and budgets of nutrients in the Bohai sea. *Journal of Ocean University of Qingdao*, *1*(1), 29–37. https://doi.org/10.1007/s11802-002-0027-3

Zhao, T.-L., Gong, S.-L., Zhang, X.-Y., & McKendry, I. G. (2003). Modeled size-segregated wet and dry deposition budgets of soil dust aerosol during ACE-Asia 2001: Implications for trans-Pacific transport. *Journal of Geophysical Research*, *108*, 8665. https://doi.org/10.1029/2002JD003363